Mechanobiology in Medicine 1 (2023) 100011

Contents lists available at ScienceDirect

Mechanobiology in Medicine

journal homepage: www.sciencedirect.com/journal/mechanobiology-in-medicine

Full Length Article

Tumor state transitions driven by Gaussian and non-Gaussian noises

Mengjiao Hua [a], Yu Wu [a,b,c,*]

[a] Key Laboratory of Soft Machines and Smart Devices of Zhejiang Province and Department of Engineering Mechanics, Zhejiang University, Hangzhou, 310027, China
[b] State Key Laboratory of Fluid Power and Mechatronic Systems, Zhejiang University, Hangzhou, 310027, China
[c] Soft Matter Research Center, Zhejiang University, Hangzhou, 310027, China

ARTICLE INFO

Keywords:
Tumor state transitions
Non-Gaussian colored noise
Stochastic basin of attraction
Basin stability

ABSTRACT

Tumor state transitions between the excited (high-concentration) and nonexcited (low-concentration) basins under the Gaussian white noise and non-Gaussian colored noise are investigated via the most probable steady states (MPSS) and the first escape probability (FEP)-based stochastic basin of attraction (SBA), respectively. Reducing the non-Gaussian colored noise and then utilizing the unified colored noise approximation (UCNA), the Markov system is derived. The extremal controlling equation of stationary probability density function (SPDF) is derived to analyze the impacts of noise on transitions in terms of MPSS. The existence of the 'color' of the non-Gaussian colored noise induces the reappearance of the uncorrelated additive white noise parameter that had vanished from the extremal controlling equation, completely reversing the inability of the uncorrelated additive Gaussian white noise to operate on transitions. The FEP-dependent SBA characterizing the excited basin stability is performed to further analyze the role of noise on the likelihood of escaping to the nonexcited state. Results show that the cross-correlated noises play a dual role in regulating SBA. The increased SBA indicating more difficulty to escape to the nonexcited state reflects a worse therapeutic effect. Therefore, enhancing the negatively correlated noise intensities and augmenting the non-Gaussian noise correlation time is essential for destabilizing the excited basin and achieving optimal therapeutic efficacy.

1. Introduction

Cancer, as a common and frequently occurring disease that poses a great threat to human health and life, is still the main cause of death worldwide, even though its diagnosis and treatment levels are constantly improving [1–3]. Investigating the effect of noise on tumor growth dynamics [4–9], especially the state transition behaviors [10–14], via dynamic methods has become a hot topic in many cancer-related studies.

Noise-induced transition [15,16] usually refers to the qualitative changes in the state behaviors of the system induced by noise, which can be characterized by the change in the extrema of the SPDF (i.e., the emergence of new extremes or the disappearance of old extremes). Gaussian white noise has been widely applied for a long time for its advantage in facilitating mathematical processing and simplifying models. Gaussian white noise on its own fails to induce any effect on the extrema of SPDF when it is applied as an additive excitation. Moreover, the actual processes usually possess finite or even long correlation time, the δ-correlation of the Gaussian white noise as an idealization of the correlation of the actual processes fails to provide a good description of the real perturbations in nature. The colored noise with exponential correlation gives a more realistic description of the noise perturbation, and in the limit case where the correlation time tends to zero, the colored noise can degenerate into white noise [17–22]. With the deepening of research and experimental verification, it is found that the noise environment in practical applications is extremely complex and often presents non-Gaussian characteristics [23–28]. When the real perturbation deviates from the Gaussian distribution, the Gaussian-type assumptions appear to be out of practice. Numerous studies related to non-Gaussian noise have demonstrated that the presence of non-Gaussian noise can induce the system to behave in richer dynamics [11,29–32]. Therefore, the study of tumor state transition under non-Gaussian noise has increasingly become a research hotspot. However, to my knowledge, few studies have focused on whether the presence of non-Gaussian noise will change the situation that independent additive Gaussian white noise can

* Corresponding author. Key Laboratory of Soft Machines and Smart Devices of Zhejiang Province and Department of Engineering Mechanics, Zhejiang University, Hangzhou, 310027, China.
E-mail address: ywu@zju.edu.cn (Y. Wu).

https://doi.org/10.1016/j.mbm.2023.100011
Received 5 June 2023; Received in revised form 10 July 2023; Accepted 17 July 2023
Available online 20 July 2023

barely cause qualitative changes in the extrema. Hence, we carry out the analysis from this perspective and demonstrate that the non-Gaussian colored noise has indeed a substantial effect on the inability of Gaussian white noise on MPSS and thus contributes to the occurrence of transition induced by Gaussian white noise.

Duan et al. proposed three indexes, the most probable trajectory, first escape probability (FEP), and mean first exit time (MFET), to characterize the state transition behavior of dynamic systems [33–37]. Han et al. applied the most probable trajectory to the related analysis of state transitions induced by Gaussian white noise and non-Gaussian colored noise in the tumor immune system [38,39]. Hao et al. studied the Lévy noise-induced transition from the high-to-low concentrations in the sense of tumor evolution trajectories [40]. Noise-induced tumor state transition can be processed to the first escape event. The probability of the excited tumor state escaping to the nonexcited basin and the time to stay in the excited basin before the first escape occurs can be characterized by FEP and MFET, respectively. Tumor states with higher FEP or shorter MFET exhibit weaker stability and are more likely to undergo state escape. In our previous studies, tumor state transitions under the joint action of non-Gaussian colored noise and Gaussian colored noise as well as time delay were studied based on FEP and MFET, respectively [10,11]. Here, we first analyze the influence of Gaussian white noise and non-Gaussian colored noise on tumor state transitions through MPSS [30], and further emphasize the outstanding capability of non-Gaussian colored noise in inducing transitions from the FEP-dependent SBA [41] perspective and suggest the best strategy to facilitate the excited tumor state escaping to the unexcited state domain.

This paper is organized as follows. In Sect.2, the non-Gaussian colored noise is approximated and then the Markov system is derived by the UCNA method. The impacts of Gaussian white noise and non-Gaussian colored noise on the transition between the excited and non-excited basins are discussed in terms of the MPSS and the FEP-dependent SBA in Sects.3 and 4, respectively. Sect. 5 gives a brief conclusion.

2. Model statement

The enzyme kinetic model [6,42] is used to study tumor growth under immune surveillance:

$$\begin{aligned}&\text{Normal Cells}\xrightarrow{\gamma} X,\\ &X\xrightarrow{\iota} 2X,\\ &X+E_0\xrightarrow{k_1}E\xrightarrow{k_2}E_0+P,\\ &P\xrightarrow{k_3},\end{aligned} \tag{1}$$

where X represents tumor cells, E_0 stands for immune cells, E denotes the mixture of X and E_0, and P represents the dead tumor cells. γ , ι , and k_i, $i=1,2,3$ are the rate coefficients. Model (1) revealing that tumor cells transformed from normal cells can undergo reproduction, decline, and eventually die can be simplified equivalently as an univariate dynamical differential equation:

$$\frac{dx_N}{d\bar{t}}=r_N x_N\left(1-\frac{x_N}{K_N}\right)-\varphi(x_N), \tag{2}$$

where x_N denotes the tumor cell populations, r_N represents the linear per capita birth rate, K_N depicts the environmental carrying capacity, and $\varphi(x_N)$ is defined as $\varphi(x_N)=\beta_N x_N^2/(A^2+x_N^2)$ to quantify the capacity of immune cells to recognize and attack tumor cells, two positive constants β_N and A are used to signify the immune coefficient and the threshold that measure whether the immune system is " switched on", respectively. The dimensions of K_N and A are the same as x_N, i.e., L^{-3}, and the dimensions of r_N and β_N are T^{-1} and $L^{-3}T^{-1}$, respectively. Introducing the non-dimensional quantities through $x=\frac{x_N}{A}$, $K=\frac{K_N}{A}$, $r=\frac{Ar_N}{\beta_N}\beta$, $t=\frac{\bar{t}\beta_N}{A}\frac{1}{\beta}$, Eq. (2) can be reduced to the following non-dimensional form:

$$\dot{x}=rx\left(1-\frac{x}{K}\right)-\frac{\beta x^2}{1+x^2}, \tag{3}$$

and a detailed explanation of parameters is given in Appendix A.

The potential function of Eq. (3) is

$$V(x)=\frac{r}{3K}x^3-\frac{r}{2}x^2+\beta(x-\arctan(x)). \tag{4}$$

As shown in Fig. 1, the tumor growth system enters the bistable region when $\beta_1<\beta<\beta_2$, where there exists an excited (disease) state with a high concentration as well as an unexcited (healthy) state with a low concentration, corresponding to the two potential wells of $V(x)$, respectively. In the presence of stochastic perturbations, state transitions between the excited and unexcited states are no longer infeasible. Appropriately modulating the noise perturbations caused by tumor microenvironmental factors (such as PH, immune status, chemical agents, radiation, etc) [43–45] to contribute to the occurrence of the excited tumor states switching to the unexcited domain, thereby turning the system state into healthy, is crucial for the clinical treatment of tumors.

We characterize the impacts of ubiquitous microenvironmental fluctuations on tumor growth with non-Gaussian colored noise and Gaussian white noise, thus introducing the stochastic tumor growth model

$$\begin{aligned}\dot{x}(t)&=f(x)+g_1(x)\varepsilon(t)+g_2(x)\xi(t)\\ \dot{\varepsilon}(t)&=-\frac{1}{\tau}\frac{d}{d\varepsilon}V_q(\varepsilon)+\frac{1}{\tau}\eta(t)\end{aligned} \tag{5}$$

with

$$\begin{aligned}f(x)&=rx\left(1-\frac{x}{K}\right)-\frac{\beta x^2}{1+x^2},\\ g_1(x)&=-x,\\ g_2(x)&=1.\end{aligned} \tag{6}$$

The non-Gaussian colored noise $\varepsilon(t)$ [26,46] given by Eq. (5) possesses the q-potential [47,48]

$$V_q(\varepsilon)=\frac{D_1}{\tau(q-1)}\ln\left[1+\frac{\tau}{D_1}(q-1)\frac{\varepsilon^2}{2}\right], \tag{7}$$

$\eta(t)$ and $\xi(t)$ are two cross-correlated Gaussian white noises with the statistic properties

$$\begin{aligned}&\langle\eta(t)\rangle=\langle\xi(t)\rangle=0,\\ &\langle\eta(t)\eta(t')\rangle=2D_1\delta(t-t'),\\ &\langle\xi(t)\xi(t')\rangle=2D_2\delta(t-t'),\\ &\langle\eta(t)\xi(t')\rangle=\langle\eta(t')\xi(t)\rangle=2\lambda\sqrt{D_1D_2}\delta(t-t').\end{aligned} \tag{8}$$

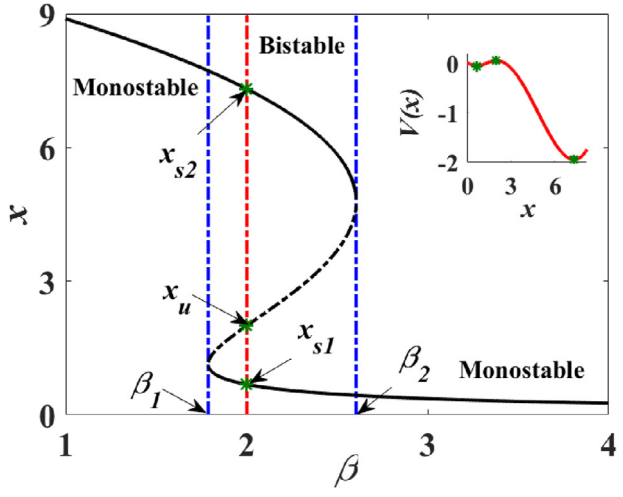

Fig. 1. Bifurcation diagram of system (3) with the bifurcation parameter β.

D_1 and D_2 are the noise intensities of $\eta(t)$ and $\xi(t)$, τ is the correlation time of $\varepsilon(t)$, q represents the deviation degree of $\varepsilon(t)$.

To obtain the Markovian approximation of system (5), we first simplify and reconstruct $\varepsilon(t)$ into a Gaussian colored noise through approximating $\frac{1}{\tau}\frac{d}{d\varepsilon}V_q(\varepsilon)$ into $\frac{\varepsilon}{\tau_{\text{eff}}}$ in the interval $|q-1| \ll 1$ [31,46,49,50]:

$$\dot{\varepsilon}(t) = -\frac{1}{\tau_{\text{eff}}}\varepsilon + \frac{1}{\tau_{\text{eff}}}\eta_1(t), \tag{9}$$

where $\eta_1(t)$ is a Gaussian noise with $\langle \eta_1(t) \rangle = 0$, $\langle \eta_1(t)\eta_1(t') \rangle = 2D_{\text{eff}}\delta(t-t')$, $D_{\text{eff}} = \left[\frac{2(2-q)}{5-3q}\right]^2 D_1$, and $\tau_{\text{eff}} = \frac{2(2-q)}{5-3q}\tau$ denotes the effective noise correlation time of the reconstructive colored noise in Eq. (9).

Subsequently, using UCNA method [46,51], the system (5) is eventually approximated as

$$\dot{x} = \tilde{f}(x) + \tilde{g}(x)\Gamma(t), \tag{10}$$

where

$$\begin{aligned}
&g(x) = \left[D_{\text{eff}}g_1^2(x) + 2\lambda\sqrt{D_{\text{eff}}D_2}\,g_1(x)g_2(x) + D_2 g_2^2(x)\right]^{1/2},\\
&f(x) = \frac{f(x)}{\nu(\tau_{\text{eff}},x)}, \tilde{g}(x) = \frac{g(x)}{\nu(\tau_{\text{eff}},x)},\\
&\nu(\tau_{\text{eff}},x) = 1 - \tau_{\text{eff}}\left[f'(x) - \frac{g_1'(x)}{g_1(x)}f(x)\right]\\
&= 1 - \tau_{\text{eff}}\frac{[-rx^4 + (K\beta - 2r)x^2 - K\beta - r]x}{K\left(1+x^2\right)^2},
\end{aligned} \tag{11}$$

$\Gamma(t)$ is a white noise with $< \Gamma(t)\Gamma(t') >= 2\delta(t-t')$.

Next, we will analyze noise-induced tumor state transitions from the perspective of MPSS and SBA to obtain the best strategy for inducing transition. Unless otherwise specified, we always set $r = 1, K = 10$, and $q = 1.1$. In addition, the UCNA regime requires that $\nu(\tau_{\text{eff}},x) > 0$, i.e., $\tau < \frac{(5-3q)K(1+x^2)^2}{2(2-q)[-rx^4+(K\beta-2r)x^2-K\beta-r]x}$, from which τ can be restricted to $\tau < 1.8017$ when $0 < x < 10$, $0 < \beta < 3$.

3. Most probable steady states (MPSS)

In this section, the maximums of SPDF (i.e., the most probable steady states) are utilized to study the influence of non-Gaussian colored noise and Gaussian white noise on tumor state transitions under immune surveillance, especially the transition from the excited domain to nonexcited domain.

The equation controlling the extremums of the SPDF corresponding to the system (10) is derived as [30].

$$m(x) - \frac{1}{2}\frac{d}{dx}\sigma^2(x) = 0, \tag{12}$$

where $m(x)$ and $\sigma(x)$ are obtained as

$$\begin{aligned}
&m(x) = \tilde{f}(x) + \tilde{g}(x)\tilde{g}'(x)\\
&= \frac{rx\left(1-\frac{x}{K}\right) - \frac{\beta x^2}{1+x^2}}{\nu(\tau_{\text{eff}},x)} + \frac{D_{\text{eff}}x - \lambda\sqrt{D_{\text{eff}}D_2}}{\nu^2(\tau_{\text{eff}},x)}\\
&- \frac{D_{\text{eff}}x^2 - 2\lambda\sqrt{D_{\text{eff}}D_2}x + D_2}{\nu^3(\tau_{\text{eff}},x)}\nu'(\tau_{\text{eff}},x),\\
&\sigma^2(x) = 2\tilde{g}^2(x)\\
&= \frac{2D_{\text{eff}}x^2 - 4\lambda\sqrt{D_{\text{eff}}D_2}x + 2D_2}{\nu^2(\tau_{\text{eff}},x)}.
\end{aligned} \tag{13}$$

We simplify the governing equation (12) as

$$\begin{aligned}
&\nu^2(\tau_{\text{eff}},x)\left(rx\left(1-\frac{x}{K}\right) - \frac{\beta x^2}{1+x^2}\right) - \nu(\tau_{\text{eff}},x)\left(D_{\text{eff}}x - \lambda\sqrt{D_{\text{eff}}D_2}\right)\\
&+\nu'(\tau_{\text{eff}},x)\left(D_{\text{eff}}x^2 - 2\lambda\sqrt{D_{\text{eff}}D_2}\,x + D_2\right) = 0.
\end{aligned} \tag{14}$$

It is worth noting that when $\tau = \lambda = 0$, Eq. (14) will be reduced to the general case that subjected to the uncorrelated Gaussian white noises, where the multiplicative noise intensity D_1 becomes the dominant parameter of MPSS, while the additive noise intensity D_2 disappears in Eq. (14), failing to cause the change in MPSS (see Fig. 2).

Fig. 2 presents the variation of MPSS with the immunity coefficient β for different noise intensities. We take x_{mb} (/ x_{ms}) to denote the MPSS in the high (/low) concentration region. In comparison with the deterministic case (red), the bistable interval in Fig. 2(a) rapidly shrinks and disappears as D_1 increases, meaning that the system eventually becomes monostable (green). Meanwhile, for the fixed β, the MPSS, especially x_{mb}, is significantly reduced. It indicates that the multiplicative Gaussian white noise fluctuation generated by the microenvironment can induce the excited tumor state under different immune surveillance conditions to escape to the nonexcited region. Moreover, the enhancement of noise intensity D_1 weakens the critical immunosurveillance conditions required for tumor state transition, thus improving the likelihood of maintaining the system state in the nonexcited state or even the tumor-free state. The alteration of the additive noise intensity D_2 in Fig. 2(b) indeed fails to exert any effect on MPSS, which is consistent with the conclusion gained from the controlling equation Eq. (14), further confirming that the uncorrelated additive Gaussian white noise alone cannot induce the occurrence of state transition.

Next, we consider the situation of $\tau \neq 0$. Fig. 3 exhibits the impacts of non-Gaussian colored noise correlation time τ on MPSS. Compared to case $\tau = 0$ with $D_1 = 0.3$ in Fig. 2(a), although enlarging τ leads to an increase in the MPSS x_{mb}, it also significantly expands the bistable range (β_1,β_2). This indicates that increasing τ can induce the system state that is always excited to enter the bistable region in advance (as reflected by the decrease of the threshold β_1) with a weaker immune surveillance intensity, which improves the possibility of staying in the nonexcited domain. Therefore, appropriately adjusting the non-Gaussian noise correlation time τ will be beneficial in reducing the required immune surveillance intensity to stay in a healthy state when combined with immunotherapy.

In contrast to the case of $\tau = 0$ in Figs. 2(b), Fig. 4 depicts the significant impact of the uncorrelated Gaussian white noise intensity D_2 on the MPSS, especially the range of the bistability region, for a large τ. The existence of nonzero τ enables the parameter D_2 that had disappeared from the controlling Eq. (14) to reappear due to the non-Markovian effect it produces, signifying that the additive white noise, aided by the non-Gaussian colored noise, not only drives the occurrence of tumor state transition but also notably reduces the critical strength of immune surveillance required for transition, exerting a beneficial role for tumor treatment.

Fig. 5 comparatively displays the influence of the noise correlation strength λ on the MPSS for different τ. The increase in λ in Fig. 5(a) causes an overall upward shift in the curve of the MPSS with β and shortens the length of the bistability interval, increasing the critical threshold of β required for state transition, which is not conducive to driving the system to the healthy state. Fig. 5(b) presents that a larger value of τ modulates the effect of λ on the MPSS in two ways: first, the enhancement of λ makes x_{mb}, which originally increased gradually, decrease significantly near the bistable region; second, the increase in τ significantly reduces the bifurcation threshold β_1, thus expanding the bistable interval and weakening the influence of λ on transition.

The above analysis reveals that the non-Markovian effect generated by the non-Gaussian noise exerts a significant influence on the noise-induced tumor state transition, especially the transition induced by the uncorrelated additive Gaussian white noise, completely reversing the situation that it has no effects on the MPSS transition at all.

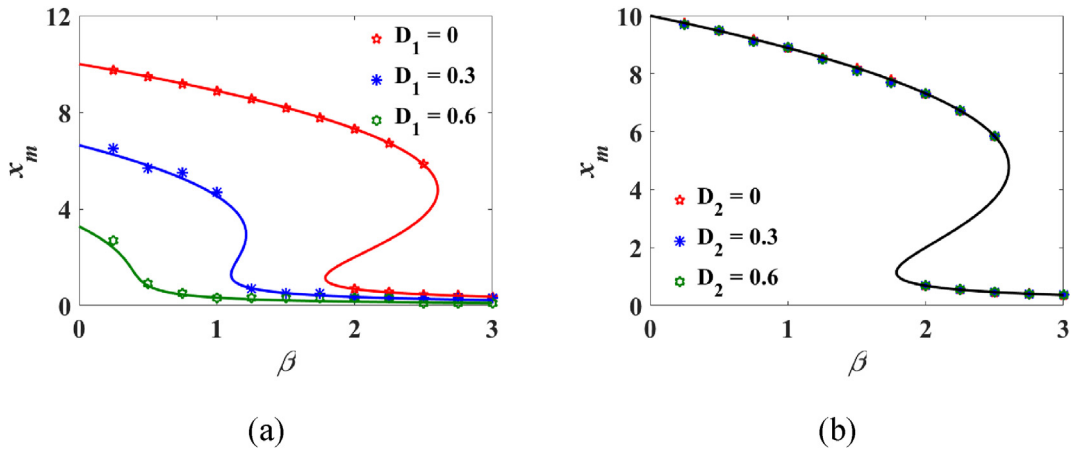

Fig. 2. The MPSS x_m versus β for different D_1 in (a) with $D_2 = 0$ and for different D_2 in (b) with $D_1 = 0$, $\tau = \lambda = 0$. Solid lines are the extremums obtained by Eq. (14), and the star markers are the MPSS obtained by MC simulations.

Next, we will further analyze the role of non-Gaussian colored noise and Gaussian white noise on the escaping behaviors of tumor states from the viewpoint of SBA.

4. Stochastic basin of attraction (SBA)

In this section, we investigate the transition between the excited (high-concentration) region $B = (x_u, x_{s2})$ and the nonexcited (low-concentration) region $B^c = (x_{s1}, x_u)$ at $\beta = 2$ by means of the SBA based on the FEP [33,34].

The FEP $P(x)$, which describes the probability of first escaping from B ($/B^c$) to B^c ($/B$) through the boundary x_u, satisfies

$$m(x)\frac{dP(x)}{dx} + \frac{1}{2}\sigma^2(x)\frac{d^2P(x)}{dx^2} = 0, x \in B(/B^c), \tag{15}$$

where

$$\begin{aligned} &P(x)|_{x_{s2}(/x_{s1})} = 0, \\ &P(x)|_{x_u} = 1. \end{aligned} \tag{16}$$

A higher FEP signifies an easier state transition, which also reflects a less stable escape region. Based on FEP, the SBA $\mathfrak{B}(p_1^*, p_2^*) \triangleq E_I \cup E_{II}$ (Fig. 6) is introduced as the set of tumor initial concentrations that meets the following criteria [34,41]:

Criterion I: $P_E(x) < p_1^*$, which gives $E_I = \{x \in B | P_E(x) < p_1^*\}$, where $P_E(x)$ is the FEP from B to B^c through x_u;

Criterion II: $P_R(x) > p_2^*$, which gives $E_{II} = \{x \in E_I^c | P_R(x) > p_2^*\}$, where $P_R(x)$ is the FEP from E_I^c ($E_I^c = B^c \cup (B - E_I)$) to E_I through x_{c1} ($P_E(x_{c1}) = p_1^*$), satisfying

$$\begin{aligned} &m(x)\frac{dP_R(x)}{dx} + \frac{1}{2}\sigma^2(x)\frac{d^2P_R(x)}{dx^2} = 0, x \in E_I^c, \\ &P_R(x)|_{x_{c1}} = 1, \\ &P_R(x)|_{x_{s1}} = 0. \end{aligned} \tag{17}$$

The larger SBA means a wider range of initial states that are difficult to escape the excited domain but easier to return from outside with a higher probability. Namely, the more stable the excited domain becomes, and thus the system is harder to get out of the disease state, leading to a poorer therapeutic effect, which needs to be avoided during tumor treatment. Moreover, we appropriately set $p_1^* = 0.6$ and $p_2^* = 0.8$ to quantify the SBA.

Fig. 7(a) depicts the FEP $P_E(x)$ in the escape region B under the influence of non-Gaussian noise intensity D_1. The reinforcement of D_1 decelerates the descent of P_E with the initial concentration x, thus inducing the critical initial state $x_{c1}|_{P_E(x_{c1})=p_1^*}$ to shift rapidly toward x_{s2}. According to Criterion I, E_I is obtained as $E_I = (x_{c1}, x_{s2})$, and accordingly, $E_I^c = (x_{s1}, x_{c1})$. The above phenomenon indicates that the enhanced D_1 significantly reduces the size of E_I, allowing more excited initial concentrations to escape to the nonexcited basin B^c with high probability, thus weakening the excited basin stability and facilitating the elimination of tumor cells. Fig. 7(b) shows the trend of $P_R(x)$ from E_I^c to E_I through x_{c1}

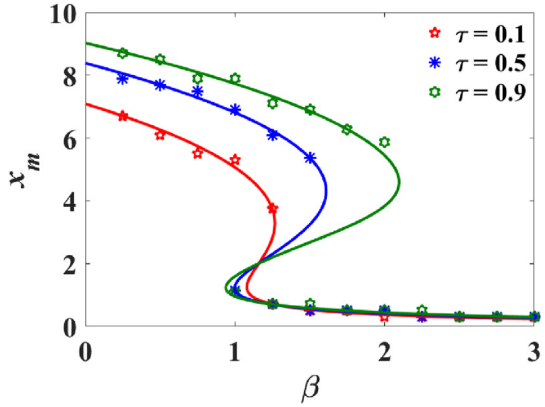

Fig. 3. The MPSS x_m versus β for different τ with $D_1 = 0.3$, $D_2 = \lambda = 0$. Solid lines are the extremums obtained by Eq. (14), and the star markers are the MPSS obtained by MC simulations.

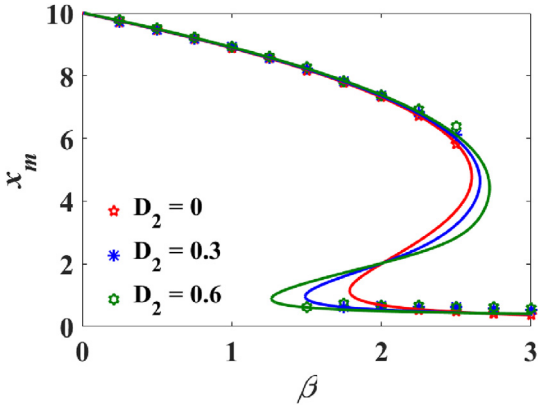

Fig. 4. The MPSS x_m versus β for different D_2 with $\tau = 0.9$, $D_1 = \lambda = 0$. Solid lines are the extremums obtained by Eq. (14), and the star markers are the MPSS obtained by MC simulations.

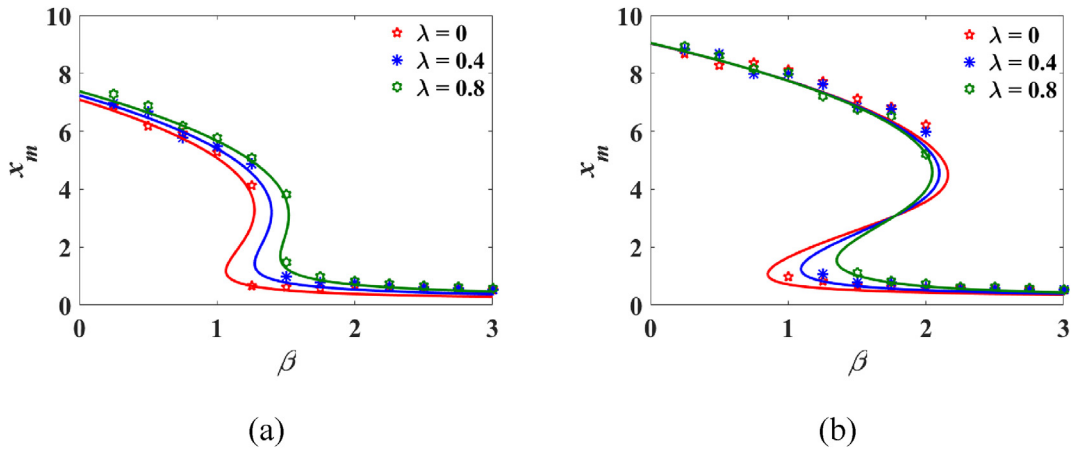

Fig. 5. The MPSS x_{m} versus β for different λ with (a) $\tau = 0.1$, (b) $\tau = 0.9$, $D_1 = D_2 = 0.3$. Solid lines are the extremums obtained by Eq. (14), and the star markers are the MPSS obtained by MC simulations.

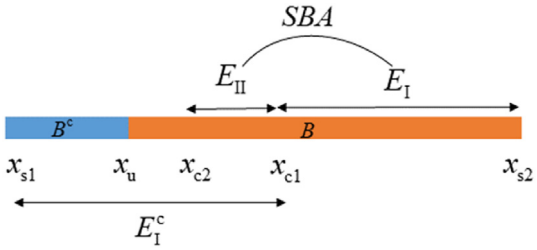

Fig. 6. Schematic diagram of tumor state transition between the excited (diseased) basin B and the nonexcited (healthy) basin B^{c}.

under the influence of D_1. In contrast to the positive dependence of P_{E} on D_1 in Fig. 7(a), P_{R} presents a non-monotonic dependence on D_1 in the region $E_{\mathrm{I}}^{\mathrm{c}}$. According to Criterion II, the critical state $x_{c2}|_{P_{\mathrm{R}}(x_{c2})=p_2^*}$ gives the left boundary of E_{II}, thus, $E_{\mathrm{II}} = (x_{c2}, x_{c1})$. Combining E_{I} and E_{II}, we obtain the SBA as $\mathfrak{B}(p_1^*, p_2^*) = (x_{c2}, x_{s2})$, that is, the position of x_{c2} controls the size of SBA. The enhancement of D_1 significantly increases x_{c2}, thereby shrinking the SBA, indicating that the stability of the high-concentration basin is weakened as a result of reinforcing the perturbation intensity generated by the microenvironmental factors, thus promoting the system state to becoming healthy and improving the tumor therapy effects.

Fig. 8 describes the effects of Gaussian white noise intensity D_2 on the FEP $P_{\mathrm{E}}(x)$ and $P_{\mathrm{R}}(x)$ in its corresponding escape region. Compared with the $P_{\mathrm{E}}(x)$ under the non-Gaussian noise intensity D_1 in Fig. 7(a), $P_{\mathrm{E}}(x)$ in Fig. 8(a) decreases faster, and the critical concentration x_{c1} in Fig. 8(a) is obviously smaller than that in Fig. 7(a) (see the boundary x_{c1} of E_{I} in Table 1) under the same increment of noise intensity, resulting in a slow shrinkage of E_{I}. In addition, $P_{\mathrm{R}}(x)$ in Fig. 8(b) increases more slowly with the initial concentration under the effect of D_2 than that under the effect of D_1 in Fig. 7(b), which makes the growth of the critical concentration x_{c2} in Fig. 8(b) smaller than that in Fig. 7(b) under the influence of the same noise intensity increment (see the boundary x_{c2} of E_{II} in Table 1). Combining the effects of D_2 on P_{E} and P_{R}, we finally conclude that the contribution of Gaussian white noise to narrowing the SBA, weakening the stability of the excited basin, and promoting the escape of the excited tumor state to the nonexcited domain is significantly weaker than that of non-Gaussian colored noise.

Next, a stability index $\delta_{\mathrm{SBA}} = L_{\mathrm{SBA}}/L_{\mathrm{B}}$ (L denotes the interval length in $\mathbb{R}^1$) is introduced to deeply analyze the effects of correlated non-Gaussian colored noise and Gaussian white noise on tumor state translation in terms of basin stability. A larger L_{SBA} indicates a more stabilized excited basin, followed by a harder escape from the disease state and a worse efficacy of tumor treatment.

Fig. 9(a) exhibits the variation of δ_{SBA} with the noise intensity D_1 under different noise correlation strength λ. For $\lambda \leq 0$, δ_{SBA} decreases with enhancing D_1, and the smaller λ hastens the decline of δ_{SBA}. That is, strengthening the non-Gaussian noise intensity contributes positively to weakening the excited basin stability and facilitating the switching to the nonexcited state. Meanwhile, strengthening the negative correlation strength (i.e., the smaller the value of λ) amplifies the significant contribution of D_1 in promoting transition. For the case $\lambda > 0$, δ_{SBA} behaves

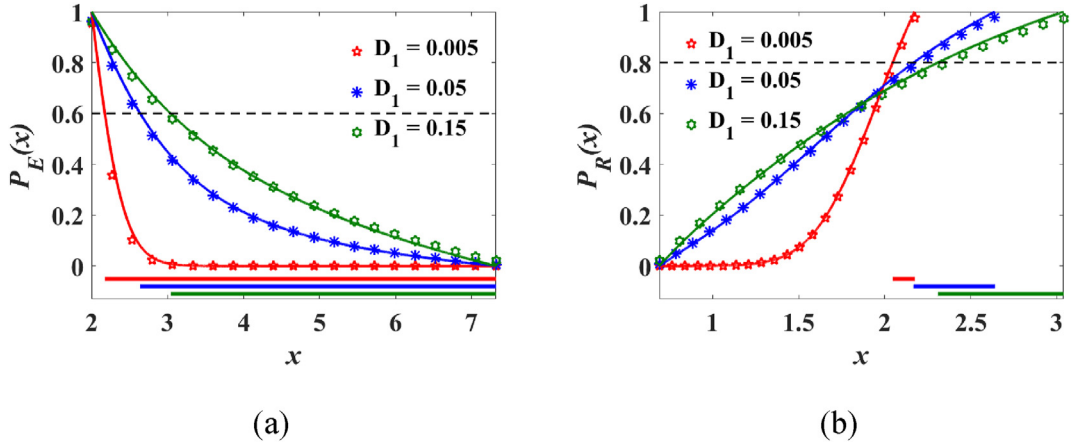

Fig. 7. Effects of D_1 on the FEP $P_{\mathrm{E}}(x)$ in (a) and $P_{\mathrm{R}}(x)$ in (b) with $D_2 = 0.005$, $\tau = 0.1$, $\lambda = 0$. Solid lines are the results obtained by Eqs. 15–17, and the star markers are the FEP obtained by MC simulations.

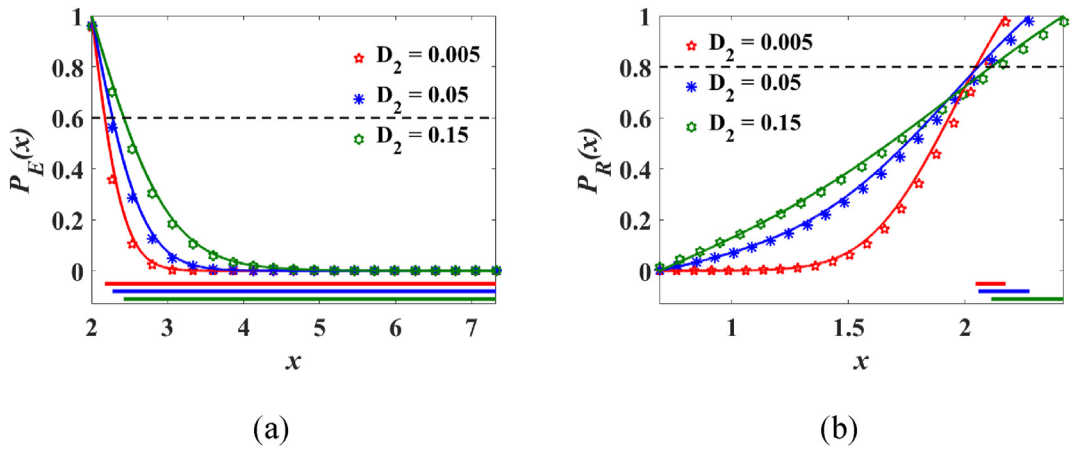

Fig. 8. Effects of D_2 on the FEP $P_{\mathrm{E}}(x)$ in (a) and $P_{\mathrm{R}}(x)$ in (b) with $D_1 = 0.005$, $\tau = 0.1$, $\lambda = 0$. Solid lines are the results obtained by Eqs. 15–17, and the star markers are the FEP obtained by MC simulations.

Table 1
Horizontal coordinate of $E_{\mathrm{I}} = (x_{c1}, x_{s2})$ and $E_{\mathrm{II}} = (x_{c2}, x_{c1})$.

Intensity	$D_1 = 0.005$	$D_1 = 0.05$	$D_1 = 0.15$	$D_2 = 0.005$	$D_2 = 0.05$	$D_2 = 0.15$
E_{I}	(2.17,7.32)	(2.64,7.32)	(3.04,7.32)	(2.17,7.32)	(2.28,7.32)	(2.42,7.32)
E_{II}	(2.05,2.17)	(2.17,2.64)	(2.31,3.04)	(2.05,2.17)	(2.06,2.28)	(2.11,2.42)

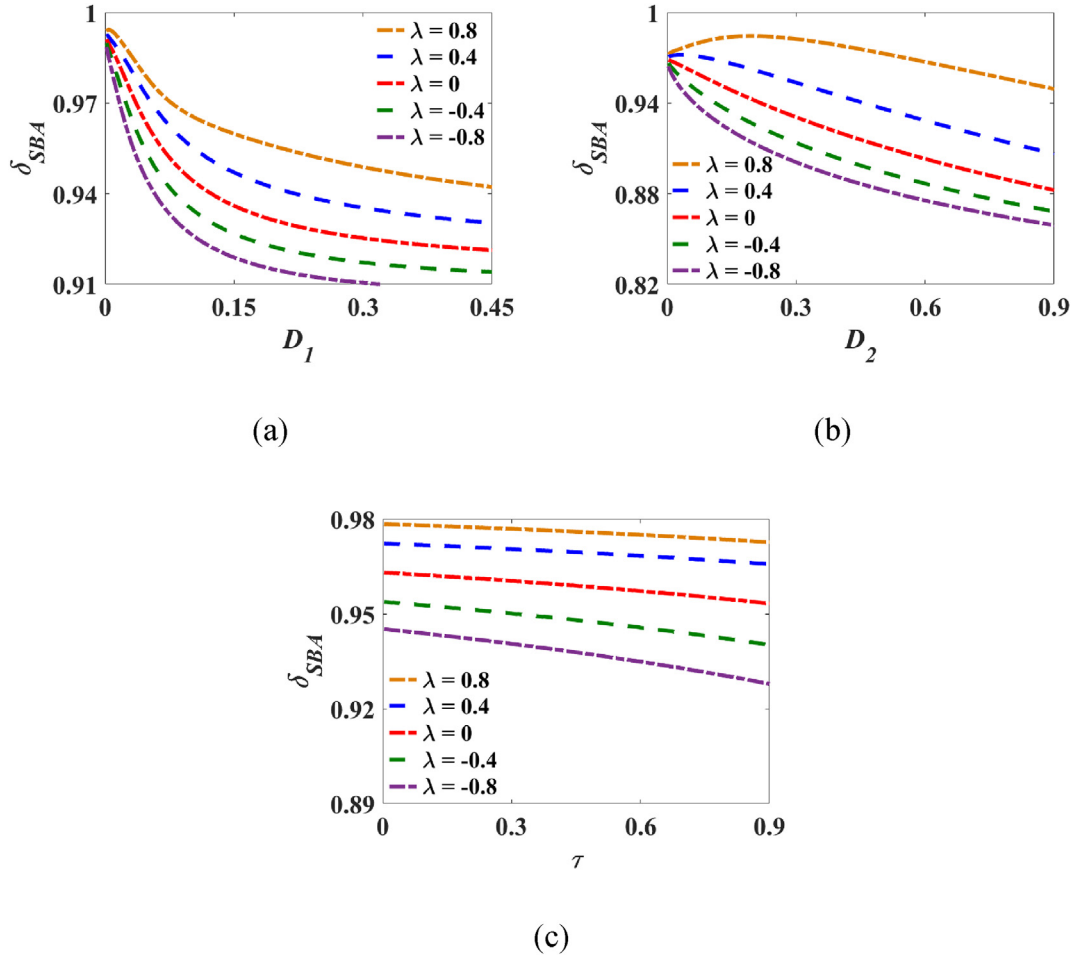

Fig. 9. Stability index δ_{SBA} under the combined influence of noise parameters, where $\tau = 0.1$, (a) $D_2 = 0.05$, (b) $D_1 = 0.05$, (c) $D_1 = D_2 = 0.05$.

nonlinearly with increasing D_1. The emergence of a critical intensity to maximize δ_{SBA} signifies enhanced excited basin stability with the lowest likelihood of state transition. Moreover, increasing the positive correlation strength mitigates the nonmonotonic variations of δ_{SBA}, thus expanding the scope of noise intensity unfavorable to state transition and should be eschewed within the tumor elimination stage. Fig. 9(b) displays δ_{SBA} versus D_2 with different λ. Compared with Fig. 9(a), δ_{SBA} varies relatively slowly with D_2, reflecting a weaker sensitivity of δ_{SBA} alterations in D_2 than to those in D_1. Therefore, adjusting the non-Gaussian noise perturbation can achieve better efficacy under the same intervention strength. Fig. 9(c) shows the opposite trends exhibited by δ_{SBA} along with increasing τ and λ. The decline of δ_{SBA} caused by τ facilitates the escaping to the nonexcited basin. However, strengthening λ diminishes the beneficial impact of τ on weakening the excited basin stability and inducing transition. Consequently, strengthening the negatively correlated noise intensities (especially the non-Gaussian colored noise intensity) and prolonging the correlation time are the preferred treatment strategies.

5. Conclusion

Tumor state transitions under the non-Gaussian colored noise and Gaussian white noise are investigated via the MPSS and SBA, respectively. We approximate the non-Gaussian colored noise to a renormalized Gaussian colored noise and then derive the Markovian approximation of the system by the UCNA. The extremal controlling equation of SPDF is derived to analyze the impacts of noise on the tumor state transition in terms of the MPSS. Subsequently, the FEP-dependent SBA is performed to characterize the stability of the excited domain, thereby reflecting the likelihood of escaping to the nonexcited state.

The results show that (i) the non-Markovian effect generated by the nonzero correlation time of the non-Gaussian colored noise enables the reappearance of the uncorrelated additive white noise parameter that had vanished from the extremal controlling equation, implying that the existence of the 'color' of the non-Gaussian colored noise completely alters the situation that the uncorrelated additive Gaussian white noise fails to act on the tumor state transition. (ii) The cross-correlated noises play a dual role in regulating the SBA. The increased SBA indicates the enhanced excited basin stability, which reflects the more difficulty to escape to the nonexcited state. Therefore, enhancing the negatively correlated noise intensities and augmenting the non-Gaussian noise correlation time is essential for promoting the turnaround of the system state to be healthy and achieving optimal therapeutic efficacy.

Previous studies on tumor state transitions mostly focused on the qualitative changes in the extreme values of SPDF induced by noise as well as the transition times between the excited and unexcited tumor states or tumor-free states, where Gaussian noise was usually utilized to emulate environmental perturbations [6,52–54]. As an additive excitation, Gaussian white noise alone is incapable of causing an effect on the extrema. In recent years, dynamical phenomena related to non-Gaussian noise have been studied extensively [55,56]. However, to my knowledge, few studies have focused on whether the existence of non-Gaussian noise will contribute substantially to changing the non-action of independent additive Gaussian white noise on the extrema of SPDF. Here we present the analysis from this perspective and show that the non-Gaussian colored noise does improve the inability of Gaussian white noise on MPSS and further highlights the superior ability of non-Gaussian colored noise to induce transitions from the SBA perspective. It is expected that this study will provide new mindsets for tumor clinical treatment.

Declaration of competing interest

The authors declare that they have no known competing financial interests or personal relationships that could have appeared to influence the work reported in this paper.

Acknowledgements

This work was supported by the Zhejiang Provincial Natural Science Foundation of China (No. LR20A020001), and the National Natural Science Foundation of China (Nos. 11932017, 11402227, 11432012, and 11621062).

Appendix A

Table 2
Description of the variables used in the paper.

Symbol	Comments
x	Population of tumor cells
r	Linear per capita birth rate of tumor cells
K	Carrying capacity of the microenvironment
β	Immune coefficient
$\varepsilon(t)$	Non-Gaussian colored noise
τ	Correlation time of $\varepsilon(t)$
q	Deviation of $\varepsilon(t)$ from the Gaussian behavior
D_1	Noise intensity of $\varepsilon(t)$
$V_q(\varepsilon)$	q-based potential of $\varepsilon(t)$
$\xi(t)$、 $\eta(t)$	Gaussian white noise
D_2	Noise intensity of $\xi(t)$

References

[1] R.A. Lake, B.W.S. Robinson, Immunotherapy and chemotherapy—a practical partnership, Nat. Rev. Cancer 5 (5) (2005) 397–405.
[2] W.A. Schulz, C. Steinhoff, A.R. Florl, Methylation of Endogenous Human Retroelements in Health and disease[J], DNA Methylation: Development, Genetic Disease and Cancer, 2006, pp. 211–250.
[3] A. Jemal, F. Bray, M.M. Center, et al., Global cancer statistics, A Cancer J. Clinic. 61 (2) (2011) 69–90.
[4] W.R. Zhong, Y.Z. Shao, Z.H. He, Spatiotemporal fluctuation-induced transition in a tumor model with immune surveillance, Phys. Rev. 74 (1) (2006) 4.
[5] B.Q. Ai, X.J. Wang, G.T. Liu, et al., Fluctuation of parameters in tumor cell growth model, Commun. Theor. Phys. 40 (1) (2003) 120.
[6] W.R. Zhong, Y.Z. Shao, Z.H. He, Pure multiplicative stochastic resonance of a theoretical anti-tumor model with seasonal modulability, Phys. Rev. 73 (6) (2006).
[7] B.Q. Ai, X.J. Wang, G.T. Liu, et al., Correlated noise in a logistic growth model, Phys. Rev. 67 (2) (2003) 022903.
[8] W.L. Duan, H. Fang, C.H. Zeng, The stability analysis of tumor-immune responses to chemotherapy system with Gaussian white noises, Chaos, Solit. Fractals 127 (2019) 96–102.
[9] H. Yang, Y.S. Tan, J. Yang, Dynamic behavior of stochastic prostate cancer system with comprehensive therapy under regime switching, Appl. Math. Model. 113 (2023) 398–415.
[10] M.J. Hua, Y. Wu, Transition and basin stability in a stochastic tumor growth model with immunization, Chaos, Solit. Fractals 158 (2022) 111953.
[11] M.J. Hua, Y. Wu, Transition in a delayed tumor growth model with non-Gaussian colored noise, Nonlinear Dynam. 111 (7) (2023) 6727–6743.
[12] A. d'Onofrio, Bounded-noise-induced transitions in a tumor-immune system interplay, Phys. Rev. 81 (2) (2010) 7.
[13] P. Roman-Roman, S. Roman-Roman, J.J. Serrano-Perez, et al., Using first-passage times to analyze tumor growth delay, Mathematics 9 (6) (2021) 14.
[14] W. Guo, L.C. Du, D.C. Mei, Transitions induced by time delays and cross-correlated sine-Wiener noises in a tumor-immune system interplay, Phys. Stat. Mech. Appl. 391 (4) (2012) 1270–1280.
[15] W. Horsthemke, Noise Induced transitions[C]. Non-equilibrium Dynamics in Chemical Systems, in: Proceedings of the International Symposium, Bordeaux, France, September 3–7, Springer, 1984, pp. 150–160.
[16] W. Horsthemke, R. Lefever, Noise-induced Transitions in Physics, Chemistry, and biology, Noise-Induced Trans.: Theory Appl. Phys. Chem. Bio. (1984) 164–200.
[17] P. Hänggi, P. Jung, Colored noise in dynamical systems, Adv. Chem. Phys. 89 (2007) 239–326.
[18] Y. Jia, J.R. Li, Stochastic system with colored correlation between white noise and colored noise, Phys. Stat. Mech. Appl. 252 (3–4) (1998) 417–427.
[19] Y. Jia, X.P. Zheng, X.M. Hu, et al., Effects of colored noise on stochastic resonance in a bistable system subject to multiplicative and additive noise, Phys. Rev. 63 (3) (2001) 031107.
[20] M.M. Kl, B.J. Matkowsky, Z. Schuss, Uniform asymptotic expansions in dynamical systems driven by colored noise, Phys. Rev. 38 (5) (1988) 2605.

[21] M.M. Kłosek-Dygas, B.J. Matkowsky, Z. Schuss, Colored noise in dynamical systems, SIAM J. Appl. Math. 48 (2) (1988) 425–441.
[22] G.Y. Liang, L. Cao, D.J. Wu, Moments of intensity of single-mode laser driven by additive and multiplicative colored noises with colored cross-correlation, Phys. Lett. 294 (3–4) (2002) 190–198.
[23] K. Kanazawa, T.G. Sano, T. Sagawa, et al., Minimal model of stochastic athermal systems: origin of non-Gaussian noise, Phys. Rev. Lett. 114 (9) (2015) 090601.
[24] V. Stojanovic, N. Nedic, D. Prsic, et al., Optimal experiment design for identification of ARX models with constrained output in non-Gaussian noise, Appl. Math. Model. 40 (13–14) (2016) 6676–6689.
[25] K. Wiesenfeld, D. Pierson, E. Pantazelou, et al., Stochastic resonance on a circle, Phys. Rev. Lett. 72 (14) (1994) 2125.
[26] H.S. Wio, S. Bouzat, Stochastic resonance: the role of potential asymmetry and non Gaussian noises, Braz. J. Phys. 29 (1999) 136–143.
[27] D. Nozaki, D.J. Mar, P. Grigg, et al., Effects of colored noise on stochastic resonance in sensory neurons, Phys. Rev. Lett. 82 (11) (1999) 2402.
[28] D. Wu, S.Q. Zhu, Stochastic resonance in a bistable system with time-delayed feedback and non-Gaussian noise, Phys. Lett. 363 (3) (2007) 202–212.
[29] W. Guo, D.C. Mei, Stochastic resonance in a tumor-immune system subject to bounded noises and time delay, Phys. Stat. Mech. Appl. 416 (2014) 90–98.
[30] M.J. Hua, Y. Wu, Bifurcation in most probable phase portraits for a bistable kinetic model with coupling Gaussian and non-Gaussian noises, Appl. Math. Mech. 42 (12) (2021) 1759–1770.
[31] M.A. Fuentes, R. Toral, H.S. Wio, Enhancement of stochastic resonance: the role of non Gaussian noises, Phys. Stat. Mech. Appl. 295 (1–2) (2001) 114–122.
[32] Y. Xu, J. Feng, J.J. Li, et al., Lévy noise induced switch in the gene transcriptional regulatory system, Chaos: An Interdisciplinary J. Nonlinear Sci. 23 (1) (2013) 013110.
[33] J.Q. Duan, An Introduction to Stochastic Dynamics, Cambridge University Press, 2015.
[34] Y.Y. Zheng, L. Serdukova, J.Q. Duan, et al., Transitions in a genetic transcriptional regulatory system under Lévy motion, Sci. Rep. 6 (2016) 12.
[35] F.Y. Wu, X.L. Chen, Y.Y. Zheng, et al., Lévy noise induced transition and enhanced stability in a gene regulatory network, Chaos 28 (7) (2018) 12.
[36] Z. Cheng, J.Q. Duan, L. Wang, Most probable dynamics of some nonlinear systems under noisy fluctuations, Commun. Nonlinear Sci. Numer. Simulat. 30 (1–3) (2016) 108–114.
[37] X.L. Chen, F.Y. Wu, J.Q. Duan, et al., Most probable dynamics of a genetic regulatory network under stable Lévy noise, Appl. Math. Comput. 348 (2019) 425–436.
[38] P. Han, W. Xu, H.X. Zhang, et al., Most probable trajectories in the delayed tumor growth model excited by a multiplicative non-Gaussian noise, Chaos, Solit. Fractals 156 (2022) 9.
[39] P. Han, W. Xu, L. Wang, et al., Most probable trajectories in a two-dimensional tumor-immune system under stochastic perturbation, Appl. Math. Model. 105 (2022) 800–814.
[40] M.L. Hao, W.T. Jia, L. Wang, et al., Most probable trajectory of a tumor model with immune response subjected to asymmetric Lévy noise, Chaos, Solit. Fractals 165 (2022) 8.
[41] L. Serdukova, Y.Y. Zheng, J.Q. Duan, et al., Stochastic basins of attraction for metastable states, Chaos 26 (7) (2016) 11.
[42] R. Lefever, R. Garay, Local description of immune tumor rejection, Biomathematics Cell Kinetics 2 (1978) 333–340.
[43] D.X. Li, W. Xu, Y.F. Guo, et al., Fluctuations induced extinction and stochastic resonance effect in a model of tumor growth with periodic treatment, Phys. Lett. 375 (5) (2011) 886–890.
[44] J. Sardanyés, T. Alarcón, Noise-induced bistability in the fate of cancer phenotypic quasispecies: a bit-strings approach, Sci. Rep. 8 (1) (2018) 1027.
[45] A.S. Garanina, V.A. Naumenko, A.A. Nikitin, et al., Temperature-controlled magnetic nanoparticles hyperthermia inhibits primary tumor growth and metastases dissemination, Nanomed. Nanotechnol. Biol. Med. 25 (2020) 102171.
[46] M.A. Fuentes, H.S. Wio, R. Toral, Effective Markovian approximation for non-Gaussian noises: a path integral approach, Phys. Stat. Mech. Appl. 303 (1–2) (2002) 91–104.
[47] D.A. Stariolo, The Langevin and Fokker-Planck equations in the framework of a generalized statistical mechanics, Phys. Lett. 185 (3) (1994) 262–264.
[48] L. Borland, Ito-Langevin equations within generalized thermostatistics, Phys. Lett. 245 (1–2) (1998) 67–72.
[49] H.S. Wio, R. Toral, Effect of non-Gaussian noise sources in a noise-induced transition, Phys. Nonlinear Phenom. 193 (1–4) (2004) 161–168.
[50] S. Bouzat, H.S. Wio, New aspects on current enhancement in Brownian motors driven by non-Gaussian noises, Phys. Stat. Mech. Appl. 351 (1) (2005) 69–78.
[51] C. Li, D.J. Wu, S.Z. Ke, Bistable kinetic model driven by correlated noises: unified colored-noise approximation, Phys. Rev. 52 (3) (1995) 3228.
[52] Y.F. Guo, W. Xu, Time-delayed Logistic system driven by correlated Gaussian white noises, Acta Phys. Sin. 57 (10) (2008) 6081–6085.
[53] F.G. Li, B.Q. Ai, Fractional Gaussian noise-induced evolution and transition in anti-tumor model, Eur. Phys. J. B 85 (2) (2012) 6.
[54] P. Han, W. Xu, L. Wang, et al., Most probable dynamics of the tumor growth model with immune surveillance under cross-correlated noises, Phys. Stat. Mech. Appl. 547 (2020) 11.
[55] L. Du, Q. Guo, Z.K. Sun, Influence of non-Gaussian noise on a tumor growth system under immune surveillance, Eur. Phys. J. Spec. Top. 227 (7–9) (2018) 895–905.
[56] Y.F. Guo, T. Yao, L.J. Wang, et al., Lévy noise-induced transition and stochastic resonance in a tumor growth model, Appl. Math. Model. 94 (2021) 506–515.